

Kinetically Consistent Coarse Graining using Kernel-based Extended Dynamic Mode Decomposition

Vahid Nateghi and Feliks Nüske*

Max-Planck-Institute for Dynamics of Complex Technical Systems, Magdeburg, Germany

E-mail: nateghi@mpi-magdeburg.mpg.de, nueske@mpi-magdeburg.mpg.de

Abstract

In this paper, we show how kernel-based approximation to the Koopman generator – the kgEDMD algorithm – can be used to identify implied timescales and meta stable sets in stochastic dynamical systems, and to learn a coarse-grained dynamics on reduced variables, which retains the essential kinetic properties of the full model. The centerpiece of this study is a learning method to identify an effective diffusion in coarse-grained space by leveraging the kgEMD model for the Koopman generator. By combining this method with force matching, a complete model for the effective dynamics can be inferred. Using a two-dimensional model system and molecular dynamics simulation data of alanine dipeptide, we demonstrate that the proposed method successfully and robustly recovers the essential thermodynamic and kinetic properties of the full model. The parameters of the method can be determined using standard model validation techniques.

1 Introduction

Stochastic simulations of large-scale dynamical systems are widely used to model the behaviour of complex systems, with applications in computational physics, chemistry, materials science, and engineering. Many examples of such systems are high dimensional and subject to meta-stability, which means the system remains trapped in a set of geometrically similar configurations, while transitions to another such state are extremely rare. As a consequence, it becomes necessary to produce very long simulations in order to make statistically robust predictions. A prime example are atomistic molecular dynamics simulations (MD)¹ of macro-molecules, where meta-stability is typically caused by high energetic barriers separating deep potential energy minima². As a result, it requires specialized high-performance computing facilities to reach the required simulation times, or it may just not be feasible at all^{3,4}.

Coarse graining (CG) describes the process of replacing the original dynamical system by a surrogate model on a (much) lower-dimensional space of descriptors^{5,6}, in such a way that certain properties of the original dynamics are preserved by the surrogate model. CG models can enable scientists to achieve much longer simulation times because of the reduced computational cost, while maintaining predictive capabilities of the full-order model. Setting up a CG model typically requires the following steps: first, the choice of a linear or non-linear mapping (CG map) from full state space to a lower-dimensional space, where the latter serves as the state space of the surrogate model. Second, definition of a parametric model class for the surrogate dynamics. Finally, determination of the parameters for that model class.

The first step is crucial to the CG model's success, and has been a very active area of research for a long time, see Refs.^{4,7,8} for reviews on this topic. In this study, we are concerned with the second and mainly the third step. CG models have often been parameterized using physically intuitive functional forms of, for instance, the coarse-grained energy. More recently, much more general functional forms have been used for the CG parameters, which

are then approximated by powerful model classes, such as deep neural networks or reproducing kernels⁹⁻¹¹, which is the approach we follow in this paper. We focus on CG for reversible stochastic differential equations (SDE) with a Boltzmann-type invariant distribution, which includes most popular simulation engines in MD, e.g. Langevin dynamics. Following the projection approach from Refs.^{12,13}, we likewise parameterize the coarse-grained model as a reversible SDE, disregarding memory terms.

Concerning parameter selection, the success of machine learning (ML) in recent years has led to the development of many powerful learning schemes for the parameters of a CG model. Examples are free energy learning¹⁴, and force matching¹⁵, among others. Many of these learning methods are geared towards ensuring *thermodynamic consistency*, which means that the surrogate model is trained to sample the marginalized Boltzmann distribution in CG space, thus ensuring accurate estimation of average quantities. Ensuring faithful reproduction of kinetic properties, such as time-correlation functions or transition time scales, is a much less developed topic, see e.g.^{16,17} for prior works in this area. In this paper, we focus on recovery of the transition time scales associated to meta stable states.

Transition rates and time scales are directly related to the leading spectrum of the system's transfer or Koopman operator¹⁸⁻²¹, which is the linear operator propagating expectation values of observable functions in time. Equivalently, one may also consider the spectrum of the associated Koopman generator (Kolmogorov operator for SDEs) close to zero. This connection has been at the heart of the Markov state modeling (MSM) approach²²⁻²⁴ and many important developments based on it²⁵⁻²⁷. The *spectral matching* approach²⁸ makes use of this connection, by first parameterizing the CG model as a linear expansion using a fixed set of basis functions, and then solving a regression problem to recover the eigenvalues of the Koopman generator. This idea was formalized in Ref.²⁹, by suggesting to regress on a full matrix representation of the Koopman generator, to capture as much kinetic content as possible. The generator matrix can be estimated a priori by a data-driven algorithm called generator EDMD (gEDMD).

In this study, we significantly improve the generator-based spectral matching, by formulating the approach using kernel methods. Reproducing kernels^{30,31} offer powerful model classes which have been applied in many areas of machine learning. Kernel-based approximation of the Koopman generator (kgEDMD) was first described in Ref.³² We use the kgEDMD matrix and a (reduced and whitened) basis of kernel functions to formulate a learning problem for a generally state-dependent effective diffusion, which optimally approximates the Koopman generator. Our approach only requires simulation data of the full system, the choice of the kernel function, and measurements of the local diffusion, which is analogue to the local mean force in force matching. Combined with the latter, this approach provides complete access to the effective dynamics associated to a reversible system.

The key contributions of this work are:

- We formulate a data-based learning problem for the effective diffusion of a coarse-grained SDE. The only hyper-parameters to be tuned are those of the kernel function. The method is robust to statistical noise and ill-conditioning as it is based on a whitened and truncated kernel bases.
- We show that diffusion learning and force matching can be combined into a single pipeline to completely parameterize a coarse-grained SDE for reversible systems.
- We show that thermodynamic and kinetic consistency are achieved by the method using two test cases, a two-dimensional model system and molecular dynamics simulations of the alanine dipeptide.

The structure of the paper is as follows: we introduce the required background on SDEs, coarse graining, and Koopman operator learning in Section 2. Our kernel-based learning framework is then presented in Section 3, while the numerical examples follow in Section 4. An overview of the notation is provided in Table 1, supplementary information on simulation details and model selection is given in the Appendix.

2 Theory

In this section, we provide the necessary background on stochastic dynamics, data-driven modeling, and Koopman spectral theory.

2.1 Stochastic processes

We consider a dynamical system described by a stochastic differential equation (SDE)

$$dX_t = b(X_t)dt + \sigma(X_t)dW_t, \quad (1)$$

where $b(X_t) : \mathbb{R}^d \rightarrow \mathbb{R}^d$ is the drift vector field, $\sigma(X_t) : \mathbb{R}^d \rightarrow \mathbb{R}^{d \times d}$ is the diffusion field, and W_t is a d -dimensional Brownian motion. We sometimes refer to the diffusion covariance matrix which is denoted as $a \in \mathbb{R}^{d \times d}$:

$$a(x) = \sigma^T(x)\sigma(x). \quad (2)$$

Processes like Equation (1) are referred to as diffusion processes. A standard example commonly used in molecular modeling is overdamped Langevin dynamics

$$dX_t = -\frac{1}{\gamma}\nabla F(X_t)dt + \sqrt{2\beta^{-1}\gamma^{-1}}dB_t, \quad (3)$$

where $F : \Omega \rightarrow \mathbb{R}$ is the potential energy, $\beta = (k_B T)^{-1}$ and γ are constants corresponding to the inverse temperature and the friction, respectively. The invariant measure for X_t in Equation (3) is the Boltzmann distribution $\mu \propto \exp(-\beta F)$, and the dynamics are reversible with respect to μ . More generally, a reversible SDE with invariant measure $\mu \propto \exp(-F)$ can be parameterized in terms of the generalized scalar potential $F : \mathbb{R}^d \mapsto \mathbb{R}$, and the

diffusion covariance a , as follows³³

$$dX_t = \left[-\frac{1}{2}a(X_t)\nabla F(X_t) + \frac{1}{2}\nabla \cdot a(X_t) \right] dt + \sigma(X_t)dW_t. \quad (4)$$

We will mostly consider reversible SDEs in this paper, and make use of the parameterization in Equation (4) when formulating learning methods.

2.2 Koopman and its generator

Koopman theory^{34,35} lifts the dynamics in Equation (1) into an infinite-dimensional space of observable functions to express the dynamics linearly. More precisely, the family of Koopman operators \mathcal{K}^t for stochastic dynamics is defined as

$$\mathcal{K}^t\psi(x) = \mathbb{E}^x [\psi(X_t)] = \mathbb{E} [\psi(X_t) | X_0 = x], \quad (5)$$

where $\mathbb{E}[\cdot]$ denotes the expected value. The operators \mathcal{K}^t form a semigroup, that is $\mathcal{K}^{s+t} = \mathcal{K}^s\mathcal{K}^t$, and one can define their infinitesimal generator \mathcal{L} as the time-derivative of the expectation value

$$\mathcal{L}\psi(x) = \frac{d}{dt}\mathbb{E}^x [\psi(x_t)]|_{t=0}. \quad (6)$$

Stochastic calculus shows that for smooth observable functions, the generator can be written as³³

$$\begin{aligned} \mathcal{L}\psi(x) &= b(x) \cdot \nabla\psi(x) + \frac{1}{2}a(x) : \nabla^2\psi(x) \\ &= \sum_{i=1}^d b_i(x) \frac{\partial}{\partial x_i} \psi(x) + \frac{1}{2} \sum_{i,j=1}^d a_{ij}(x) \frac{\partial^2}{\partial x_i \partial x_j} \psi(x), \end{aligned} \quad (7)$$

where a and b are the diffusion and drift terms defined above, $\nabla^2[\cdot]$ is the Hessian matrix of a function, and the colon $:$ is a short-hand for the dot product between two matrices, also

called Frobenius inner product. For overdamped Langevin dynamics, Eq. (7) simplifies to

$$\mathcal{L}\psi(x) = -\frac{1}{\gamma}\nabla F(x) \cdot \nabla\psi(x) + \frac{1}{\gamma\beta}\Delta\psi(x).$$

2.3 Spectral decomposition

A key quantity of interest are the eigenvalues and eigenfunctions of the generator. The study of spectral components of the generator helps us identify the long-time dynamics of the system. In molecular dynamics, we expect to find a number of eigenvalues close to zero, followed by a spectral gap. These low-lying eigenvalues are indicating the number of meta stable states of the system, which are the macrostates the system stays in the longest¹⁸. We write the eigenvalue problem for the generator as

$$-\mathcal{L}\psi_i = \lambda_i\psi_i. \tag{8}$$

The eigenvalues λ_i of $-\mathcal{L}$ must be non-negative, and the lowest eigenvalue $\lambda_1 = 0$ is non-degenerate under very mild conditions³⁶ $0 = \lambda_1 < \lambda_2 \leq \lambda_3 \leq \dots$. We also refer to the eigenvalues as rates, and to their reciprocals as implied timescales²²

$$t_i = \frac{1}{\lambda_i}. \tag{9}$$

2.4 Coarse graining

One of the main motivations of this work is to learn an SDE representing the full dynamics (1) on a coarse-grained space. Coarse graining (CG) is realized by mapping the state space Ω onto a lower-dimensional space $\hat{\Omega} \subset \mathbb{R}^{d_\xi}$ by means of a smooth CG function ξ . We write ν for the marginal distribution of the full-space invariant measure μ projected onto CG space. An important object is the space L_ν^2 of functions on $\hat{\Omega}$ which are square integrable with respect to the weight function ν . The space L_ν^2 is a subspace of L_μ^2 comprising all functions

that depend only on the value of ξ . Moreover, the orthogonal projector onto L_ν^2 from L_μ^2 is the *conditional expectation operator*^{12,13}

$$\mathcal{P}\psi(z) = \frac{1}{\nu(z)} \mathbb{E}^\mu[\psi(x)|\xi(x) = z], \quad (10)$$

where z is a position in CG space. This operator calculates the average of a function ψ over all $x \in \Omega$ whose projection onto CG space is the same point $z \in \hat{\Omega}$.

Considering \mathcal{P} , following the exposition in,¹³ one can define the projected generator

$$\mathcal{L}^\xi = \mathcal{P}\mathcal{L}\mathcal{P}. \quad (11)$$

It turns out its action on a function $\varphi \in L_\nu^2$ is given by

$$\mathcal{L}^\xi(\phi) = \mathcal{P}[\mathcal{L}\xi] \cdot \nabla_z \phi + \frac{1}{2} \mathcal{P}[\nabla \xi^T a \nabla \xi] : \nabla_z^2 \phi. \quad (12)$$

As one can see, \mathcal{L}^ξ is of the same form as the original generator \mathcal{L} in Equation (7), and indeed it is the generator of an SDE Z_t on $\hat{\Omega}$

$$dZ_t = b^\xi(Z_t)dt + \sigma^\xi(Z_t)dW_t. \quad (13)$$

The effective drift and diffusion coefficients are given in analytical form by

$$b^\xi(z) = \mathcal{P}(\mathcal{L}\xi)(z) \quad a^\xi(z) = \mathcal{P}(\nabla \xi^T a \nabla \xi)(z), \quad (14)$$

and the practical task of coarse graining is to approximate them numerically. An important result, shown in¹³, and that we will use later on, is that the inner product of the projected generator with respect to the invariant measure ν in CG space is equal to the inner product

of the original generator with respect to the invariant measure μ of the full space

$$\langle \mathcal{L}\psi \circ \xi, \varphi \circ \xi \rangle_\mu = \langle \mathcal{L}^\xi \psi, \varphi \rangle_\nu \quad (15)$$

where ψ and φ are functions in L^2_ν .

2.5 Dynamic mode decomposition and its extension

Dynamic Mode Decomposition (DMD) is a conceptually simple method that provides a linear map to propagate the state of a dynamical system in time. The method was originally proposed in Ref.³⁷ and since then, many variations and extensions have been proposed, see Ref.^{38,39} for an overview. Basically, DMD looks for the best-fit linear operator \mathbf{A} that advances the system state by solving the minimization problem in Equation (16)

$$\mathbf{A} = \arg \min_{\mathbf{A}'} \|\mathbf{X}^\tau - \mathbf{A}\mathbf{X}\|_F = \mathbf{X}^\tau \mathbf{X}^\dagger \quad (16)$$

where \mathbf{X} and \mathbf{X}^τ are collections of time-shifted snapshots of the dynamics, and \dagger denotes the pseudo-inverse. Although DMD is a popular and widely-used method in data-driven modeling, it can only provide a linear model and the systems we are interested in for molecular dynamics are highly nonlinear.

Improved results can be obtained by using nonlinear functions instead of just the raw state variables. This method is known as Extended DMD (EDMD)⁴⁰, that can provide more accurate models by capturing nonlinearities. After defining a dictionary of observables, $\{\psi_i\}_{i=1}^n$ (that are functions of the state space Ω), we compile the evaluations of all dictionary functions at all snapshots into matrices

$$\mathbf{\Psi} = [\psi_i(x_l)]_{i,l} \in \mathbb{R}^{n \times m}, \quad \mathbf{\Psi}^\tau = [\psi_i(x_{l+1})]_{i,l} \in \mathbb{R}^{n \times m},$$

where we assume for simplicity that subsequent snapshots are separated by time τ . We then solve the optimization problem:

$$\mathbf{K} = \arg \min_{\mathbf{K}'} \|\Psi^\tau - \mathbf{K}'\Psi\|_F = \Psi^\tau \Psi^\dagger. \quad (17)$$

The solution of Equation (17) can be obtained numerically using singular value decomposition. In the limit of infinite data, EDMD constitutes a finite-dimensional projection (Galerkin projection) of the Koopman operator onto the subspace spanned by the dictionary functions⁴⁰.

2.6 Generator EDMD

The infinitesimal generator of the Koopman operator can also be approximated by an algorithm similar to EDMD, called gEDMD²⁹. Once again, given a set of scalar basis functions $\psi(x) = \{\psi_1(x), \dots, \psi_n(x)\}$, and training data $\{x_l\}_{l=1}^m$, we form the matrices

$$\Psi = [\psi_i(x_l)]_{i,l}, \quad \mathcal{L}\Psi = [\mathcal{L}\psi_i(x_l)]_{i,l},$$

using the analytical formula (7) to evaluate the second of these matrices. Solving an analogous regression problem to (17) leads to the matrix

$$\mathbf{L}^\top = (\mathcal{L}\Psi)\Psi^\dagger = \hat{\mathbf{A}}\hat{\mathbf{G}}^{-1}, \quad (18)$$

where

$$\begin{aligned} \hat{\mathbf{A}}_{ij} &= \frac{1}{m} \sum_{k=1}^m (\mathcal{L}\psi_i)(x_k) \psi_j(x_k), \\ \hat{\mathbf{G}}_{ij} &= \frac{1}{m} \sum_{k=1}^m \psi_i(x_k) \psi_j(x_k). \end{aligned} \quad (19)$$

As for EDMD, it was proved in Ref.²⁹ that in the infinite-data limit, gEDMD converges to the Galerkin projection of the generator onto the space spanned by the basis functions

$$\mathbf{L}^\top = \mathbf{A}\mathbf{G}^{-1}, \quad \mathbf{A}_{ij} = \langle \mathcal{L}\psi_i, \psi_j \rangle_\mu \quad \mathbf{G}_{ij} = \langle \psi_i, \psi_j \rangle_\mu. \quad (20)$$

The matrices \mathbf{G} and \mathbf{A} are often called mass and stiffness matrix, respectively. For arbitrary stochastic dynamics, the computation of \mathbf{A} involves a second-order differentiation as shown in Equation (7). However, if the stochastic dynamics are reversible, only first-order derivatives are required to compute the matrix \mathbf{A} , as the generator satisfies the following integration-by-parts formula

$$\mathbf{A}_{ij} = \langle \mathcal{L}\psi_i, \psi_j \rangle_\mu = -\frac{1}{2} \int \nabla \psi_i \sigma \sigma^T \nabla \psi_j^T \, d\mu. \quad (21)$$

If the basis functions are actually defined in a CG space $\hat{\Omega}$, that is $\psi_i(x) = \psi_i(\xi(x))$, then by the chain rule the matrix A can be written as

$$\begin{aligned} \mathbf{A}_{ij} &= -\frac{1}{2} \int \nabla_x \psi_i \sigma \sigma^T \nabla_x \psi_j^T \, d\mu = -\frac{1}{2} \int (\nabla_z \psi_i \nabla_x \xi) \sigma \sigma^T (\nabla_x \xi^T \nabla_z \psi_j^T) \, d\mu \\ &= -\frac{1}{2} \int (\nabla_z \psi_i) (\nabla_x \xi \sigma \sigma^T \nabla_x \xi^T) (\nabla_z \psi_j^T) \, d\mu. \end{aligned} \quad (22)$$

We refer to the matrix

$$a_{\text{loc}}^\xi(x) = \nabla_x \xi \sigma \sigma^T \nabla_x \xi^T \in \mathbb{R}^{d_\xi \times d_\xi} \quad (23)$$

as *local diffusion*, and note that it is independent of the basis functions. It can therefore be computed a priori in numerical calculations.

3 Methods

3.1 Overview and Notation

Successful application of the gEDMD method requires selecting proper and expressive basis functions. This is not a trivial task and can highly depend on the dynamics of interest. To

alleviate this, use of kernel methods has been proposed in Ref.³². The *kgEDMD* method is based on choosing the basis functions as *features* of a reproducing kernel $k(x, y)$ at the training data:

$$\Phi = [k(\cdot, x_1), k(\cdot, x_2), \dots, k(\cdot, x_m)]^\top. \quad (24)$$

We consider Φ as a vector-valued function, that is, we write

$$\Phi(x) = [k(x, x_1), k(x, x_2), \dots, k(x, x_m)]^\top \quad (25)$$

for the m -dimensional vector obtained by evaluating all the kernel features at x . Since kernels are two-argument functions, we can take their derivatives with respect to both arguments, and in fact we will need to distinguish these derivatives when formulating our methods. In general, we simply write $\nabla_1 k$ and $\nabla_2 k$ for gradients of the kernel function with respect to its first and second argument. Similarly, we write $\nabla_1 \Phi$, $\nabla_2 \Phi$ for the matrix-valued functions we obtain by assembling the gradients of all kernel features:

$$\nabla_1 \Phi(x) = \begin{bmatrix} \nabla_1 k(x, x_1) \\ \vdots \\ \nabla_1 k(x, x_m) \end{bmatrix} \in \mathbb{R}^{m \times d}, \quad \nabla_2 \Phi(x) = \begin{bmatrix} \nabla_2 k(x, x_1) \\ \vdots \\ \nabla_2 k(x, x_m) \end{bmatrix} \in \mathbb{R}^{m \times d}. \quad (26)$$

One of the widely used kernel functions is the Gaussian kernel given by

$$k(x_i, x_j) = \exp\left(-\frac{\|x_i - x_j\|^2}{2\sigma^2}\right), \quad (27)$$

where σ is the standard deviation or bandwidth of the Gaussian kernel. If the state space is a periodic domain, we make use of a periodic Gaussian kernel instead⁴¹

$$k(x_i, x_j) = \exp\left(-\frac{\sum_{i=1}^d \sin\left(\frac{\pi}{p}(x_i - x_j)\right)^2}{2\sigma^2}\right), \quad (28)$$

where σ is again the bandwidth of the Gaussian kernel, p is the half-period of the domain, and d is the dimension of system.

3.2 Kernel-based Koopman generator EDMD

Using the kernel feature basis as in Equation (24), we can seek a data-driven approximation to the eigenfunctions of the Koopman generator in the form $\psi_i(x) = \mathbf{u}_i^\top \Phi(x)$. As detailed in Ref.³², the coefficient vectors \mathbf{u}_i , are then found as solutions of the following generalized matrix eigenvalue problem

$$\hat{\mathbf{A}}\mathbf{u}_i := \frac{1}{2} \sum_{l=1}^d (\hat{\mathbf{A}}^{(l)})^\top \hat{\mathbf{A}}^{(l)} \mathbf{u}_i = \hat{\lambda}_i \hat{\mathbf{G}} \hat{\mathbf{G}} \mathbf{u}_i, \quad (29)$$

where d is the dimension of the state space. The matrices $\hat{\mathbf{A}}^{(l)}$ and $\hat{\mathbf{G}}$ are based on the reversible formulation for *gEDMD*, and essentially contain pairwise evaluations of the kernel and its first-order derivatives

$$\begin{aligned} \left[\hat{\mathbf{G}} \right]_{ns} &= k(x_n, x_s) \\ \left[\hat{\mathbf{A}}^{(l)} \right]_{ns} &= \sigma_l(x_n)^\top \nabla_2 k(x_n, x_s). \end{aligned} \quad (30)$$

The kernelized mass matrix $\hat{\mathbf{G}}$ is often highly ill-conditioned. Therefore, we compute a reduced generator by performing a whitening transformation based on removing small eigenvalues of the mass matrix

$$\hat{\mathbf{G}} = \mathbf{U} \Sigma \mathbf{U}^\top, \quad \mathbf{R} = \mathbf{U} \Sigma^{-0.5} \in \mathbb{R}^{m \times r}, \quad \hat{\mathbf{L}}_r = \mathbf{R}^\top \hat{\mathbf{A}} \mathbf{R}, \quad (31)$$

in which $r \leq m$. Here, \mathbf{R} is a transformation matrix mapping the original basis built by the feature map Φ , to the reduced basis

$$\mathbf{h}(x) = \mathbf{R}^\top \Phi(x) \in \mathbb{R}^r. \quad (32)$$

In preparation for later, we also introduce the notation

$$\nabla \mathbf{h}(x) = [\partial_j h_l(x)]_{l,j} = \mathbf{R}^\top \nabla_1 \Phi(x) \in \mathbb{R}^{r \times d} \quad (33)$$

for the gradients of all reduced features evaluated at point x . Diagonalization of the reduced generator matrix $\hat{\mathbf{L}}_r$ then provides the final estimates for the generator’s eigenvalues and eigenfunctions.

3.3 System identification

The reduced generator matrix $\hat{\mathbf{L}}_r$ provides an empirical model for the Koopman generator \mathcal{L} on the space of whitened and rank-reduced features \mathbf{h} . Hence we can use this model towards other ends besides identification of the meta stable sets. Among other purposes, we can use it to identify an effective SDE governing the CG dynamics as in Equation (13), using a procedure that was already sketched in Ref.²⁹. We parameterize the CG dynamics as a reversible SDE, which is justified if the original dynamics are reversible¹³. As discussed in Section 2 and in Ref.³³, reversible systems can be characterized by the diffusion $a^\xi \in \mathbb{R}^{d_\xi \times d_\xi}$ and a scalar potential $F^\xi : \mathbb{R}^{d_\xi} \rightarrow \mathbb{R}$, from which the drift is then obtained by:

$$b^\xi = -\frac{1}{2} a^\xi \nabla_z F^\xi + \frac{1}{2} \nabla \cdot a^\xi. \quad (34)$$

Thus, to identify the SDE, we need to learn these two components, which can be broken up into two separate problems. From now on, we employ a kernel k on the CG space $\hat{\Omega}$, that is $k = k(z, z')$.

3.3.1 Force matching

Knowing the full-process scalar potential field F and the CG function ξ , the effective force can be obtained by a well-known technique called *force matching*¹⁵ via the following minimization

problem

$$\nabla_z F^\xi = \arg \min_{g \in L^2_\nu} \frac{1}{m} \sum_{i=1}^m \left\| g(\xi(x_i)) - f_{\text{lmf}}^\xi(x_i) \right\|^2, \quad (35)$$

where m is the data size and f_{lmf}^ξ is called *local mean force* and defined as follows

$$\begin{aligned} f_{\text{lmf}}^\xi &= -\nabla_x F \cdot G^\xi + \nabla_x \cdot G^\xi \\ G^\xi &= \nabla_x \xi [(\nabla_x \xi)^T \nabla_x \xi]^{-1}. \end{aligned} \quad (36)$$

In line with the kernel-based approach we follow in this work, we parameterize the optimal vector field g as the gradient of a linear combination of the feature basis Φ in Equation (24)

$$F^\xi(z) = \alpha^\top \Phi(z), \quad g(z) = \alpha^\top \nabla_1 \Phi(z) = \sum_{i=1}^m \alpha_i \nabla_1 k(z, z_i). \quad (37)$$

The force matching problem thus breaks down to determination of m optimal expansions coefficients α . We stress, however, that any other parameterization could be used for this step, for example a deep learning-based method¹¹.

3.3.2 Kernel-based diffusion learning

Our main contribution is a learning method for the effective diffusion, complementing the effective potential F^ξ . We first use training data of the full space dynamics and the kernel k on the CG space $\hat{\Omega}$, to learn a reduced matrix representation $\hat{\mathbf{L}}_r$ of the full generator. Recalling Equation (15), the matrix $\hat{\mathbf{L}}_r$ is at the same time an approximation to the CG generator \mathcal{L}^ξ . On the CG space, the reversible generator \mathcal{L}^ξ also satisfies the integration-by-parts formula (21),

$$\langle \mathcal{L}^\xi \psi, \varphi \rangle_\nu = -\frac{1}{2} \int_{\hat{\Omega}} \nabla_z \psi(z) a^\xi(z) \nabla_z \varphi(z)^\top d\nu(z), \quad (38)$$

which only features an explicit dependence on the unknown effective diffusion a^ξ , see Equation (14). Using the reduced basis $\mathbf{h}(z) = \mathbf{R}^\top \Phi(z)$, we parameterize the effective diffusion as

$$\sigma_\alpha^\xi(z) = \sum_{l=1}^r \alpha_l h_l(z), \quad (39)$$

where, in the most general case, $\alpha_l \in \mathbb{R}^{d_\xi \times d_\xi}$ must be matrix-valued coefficients. To arrive at a compact expression, we gather all unknown expansion coefficients α_l as a third order tensor $\alpha \in \mathbb{R}^{d_\xi \times d_\xi \times r}$, which allows us to write

$$\sigma_\alpha^\xi(z) = \alpha \cdot_{|3,1} \mathbf{h}(z) = \alpha \cdot_{|3,1} \mathbf{R}^\top \Phi(z), \quad (40)$$

using the notation $\mathbf{a} \cdot_{|i,j} \mathbf{b}$ to denote contraction of two tensors \mathbf{a} , \mathbf{b} over indices i and j of commensurate dimension. Plugging this into Equation (38) and using the data-driven estimator of Equation (30), we obtain a parametric model for the reduced generator matrix $\hat{\mathbf{L}}_r$

$$\begin{aligned} [\hat{\mathbf{L}}_\alpha^\xi] &= \frac{1}{2m} \sum_{k=1}^m \nabla \mathbf{h}(z_k) \sigma_\alpha^\xi(z_k) \sigma_\alpha^\xi(z_k)^\top \nabla \mathbf{h}^\top(z_k) \\ &= \frac{1}{2m} \sum_{k=1}^m \mathbf{S}^\alpha(z_k) \mathbf{S}^\alpha(z_k)^\top, \end{aligned} \quad (41)$$

$$\mathbf{S}^\alpha(z) := \nabla \mathbf{h}(z) \sigma_\alpha^\xi(z).$$

Combining Equations (33) and (40), we can compactly write

$$\mathbf{S}^\alpha(z) = \mathbf{R}^\top \nabla_1 \Phi(z) \alpha \cdot_{|3,1} \mathbf{R}^\top \Phi(z), \quad (42)$$

which is now expressed solely in terms of the kernel features Φ , the whitening transformation \mathbf{R} , and the unknown coefficient tensor α . We then learn the effective diffusion by matching the parameterized generator matrix $\hat{\mathbf{L}}_\alpha^\xi$ to the true reduced generator matrix $\hat{\mathbf{L}}_r$, therefore

solving the following minimization problem:

$$\alpha^* = \arg \min_{\alpha \in \mathbb{R}^{d_\xi \times d_\xi \times r}} \left[\left\| \hat{\mathbf{L}}_r - \hat{\mathbf{L}}_\alpha^\xi \right\|_2^2 + \gamma \left\| \frac{\partial \sigma}{\partial z} \right\|_2^2 \right], \quad (43)$$

where $\hat{\mathbf{L}}_\alpha^\xi$ is calculated from α via Equations (41) and (42). To avoid over-fitting and to suppress oscillations in σ , we found that introducing the second term to regularize the derivatives of the diffusion provides the best results.

Here, the effective diffusion is represented by a full matrix. However, for simplicity, we only learn a diagonal diffusion matrix for the numerical results reported in the following section. The method can be summarized in Algorithm 1.

Algorithm 1 Learning Effective Dynamics with kgEDMD

Input: full space data $\{x_k\}_{k=1}^m$ in \mathbb{R}^d , CG map ξ , kernel function k ,
Truncation rule for r in Equation (31), regularization γ

- 1: Diffusion learning
 - 2: Compute local diffusion a_{loc}^ξ as in Equation (23).
 - 3: Form mass and stiffness matrices \mathbf{G} and $\mathbf{A}^{(l)}$ as in Equation (30)
 - 4: Compute reduced generator $\hat{\mathbf{L}}_r$ as in Equation (31)
 - 5: Perform the minimization problem as in Equation (43)
 - 6: Form the effective diffusion σ_α^ξ as in Equation (39)
 - 7: Force matching
 - 8: Compute the local mean force f_{lmf}^ξ as in Equation (36)
 - 9: Perform the minimization problem as in Equation (35)
 - 10: Form the effective potential F^ξ as in Equation (37)
-

4 Examples

To show the effectiveness of the proposed method, we apply it to a two-dimensional model system defined by the Lemon-slice potential, and to MD simulation data of the alanine dipeptide, which is a widely-used test case in molecular dynamics.

As the optimization block for diffusion learning is non-convex, we use a library function from *scipy*'s optimization toolbox, but solve the problem repeatedly for 50 randomly generated

initial guesses. The optimization block for the force matching, on the other hand, is done via ridge regression.

4.1 Lemon-Slice potential

4.1.1 System introduction

The Lemon-slice system is governed by overdamped Langevin dynamics in Equation (3) with the following potential F

$$F(x, y) = F(r, \phi) = \cos(4\phi) + 10(r - 1)^2, \quad (44)$$

where r and ϕ are polar coordinates. The energy landscape of the system is shown in Figure 1 a. To form the SDE for this example, we consider a diagonal state-dependent diffusion field $\sigma(x)$ defined as

$$\sigma(x) = \begin{bmatrix} \sqrt{\frac{2}{\beta}(\sin(\phi) + 1.5)} & 0 \\ 0 & \sqrt{\frac{2}{\beta}(\sin(\phi) + 1.5)} \end{bmatrix} \quad (45)$$

where $\beta = 1$ is the inverse temperature. Using the Euler-Maruyama scheme at discrete integration time step $dt = 10^{-3}$ for integration of the SDE, we collect the training data for learning. For the sake of validation and showing the robustness of the method, we produce 5 independent experiments, each with length of $m = 10^5$ time steps. We further down sample them to 1000 samples each for learning effective force and diffusion.

As shown in previous studies, the polar angle ϕ is a suitable CG coordinate for this system, as it resolves all four meta stable states

$$\xi(x, y) = \phi. \quad (46)$$

For this system, analytical expressions for the effective drift and diffusion along ξ can be

obtained by a slight modification of the results in⁴², and serve as reference values.

We use the kgEDMD algorithm on the reaction coordinate ξ , to identify the generator eigenvalues and meta stable states and, subsequently, to identify an effective dynamics along ξ using Algorithm 1.

As a first try, we consider the Gaussian kernel for Galerkin approximation of the generator. Notice that the CG dynamics of Lemon-slice problem is periodic in the polar angle, however, a generic Gaussian kernel is not so. Thus, it cannot capture the periodicity of the system of interest. As an alternative, we also use the periodic Gaussian kernel as in Equation (28) and analyze both. The kernel bandwidth in either versions of Gaussian kernel is optimized using cross validation based on the VAMP-score²⁷. Details on the VAMP-score analysis are reported in the appendix.

4.1.2 Meta-stability analysis

Figure 1 c shows the leading eigenvalues obtained from the kgEDMD model. As one notices, there are four dominant eigenvalues followed by a gap. These four eigenvalues are corresponding to the four minima in the potential field. Having determined the eigenvectors of the generator, we can perform robust Perron Cluster Cluster Analysis (PCCA+)⁴³ algorithm to assign to each sample point its membership to each meta stable state. Figure 1 b shows that the four potential minima are perfectly recovered in this way. A comparison of the leading eigenvalues of the reference model $\hat{\mathbf{L}}_r$ and the optimal matrix $\hat{\mathbf{L}}_\alpha^\xi$ is shown in Figure 1 c. Both choices of the kernel function lead to satisfactory results, the periodic kernel provides slightly higher accuracy in approximation of the generator eigenvalues. Note that the kernel bandwidth is tuned for each kernel function separately.

4.1.3 Identification of CG dynamics

The learned generator providing the eigenvalues reported above is built upon the effective diffusion shown in Figure 2 b, which is almost perfectly following the reference. Further-

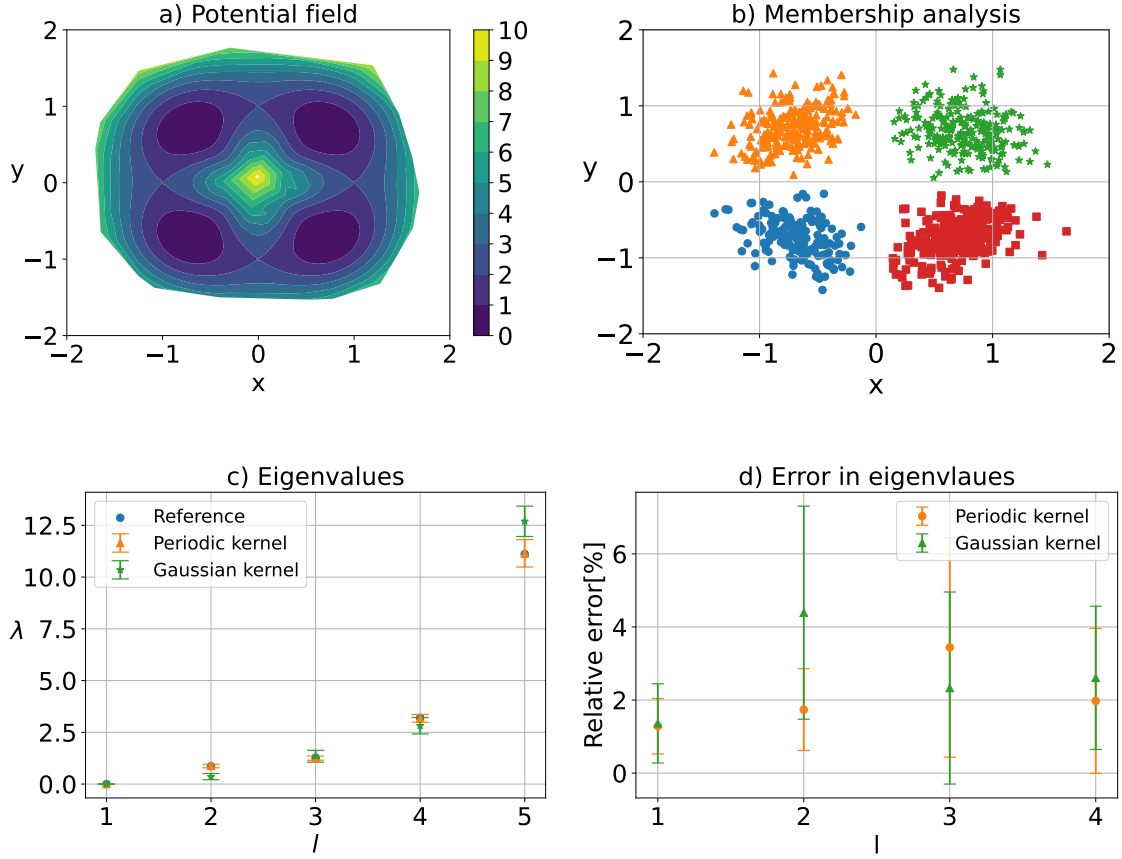


Figure 1: Approximation of generator for the Lemon slice system. Potential field in (a). Membership analysis in (b) using 1000 samples. The dominant eigenvalues of the reference generator $\hat{\mathbf{L}}_r$ and the learned generator $\hat{\mathbf{L}}_\alpha^\xi$ built upon the learned effective diffusion, using Gaussian and periodic Gaussian kernels, in (c). The relative error of these eigenvalues compared to the reference is shown in (d).

more, we perform the force matching as well and obtain the effective force in the CG space shown in Figure 2 a. From the effective force and diffusion, the effective drift can be obtained according to Equation (34), which is also compared against the analytical expression in Figure 2 c, likewise showing very good agreement.

Having effective drift and diffusion, we are able to build the learned SDE governing the CG coordinate. We use the Euler-Maruyama scheme to integrate the learned and reference SDEs with integration time step of $dt = 10^{-3}$. Figure 2 d shows two trajectories of the CG coordinate ϕ for both dynamics for 10^4 time steps, using the same Brownian motion for both trajectories. The propagated learned system follows the reference closely, with both systems staying long times in each meta stable state, and rarely swapping in between those. The results demonstrate that the proposed method can approximate the full system’s meta stable sets well, and identify a suitable SDE for CG dynamics which is accurate even on the level of individual trajectories.

In this example, both the full dynamics and the learned effective dynamics possess state-dependent diffusion fields. We compare the properties of the learned CG model with variable diffusion to those of a CG dynamics with constant diffusion. For the latter, we set the effective diffusion constant to $a = \frac{2}{\beta} = 2$. We propagate the corresponding SDEs for a sufficiently large span of time, and estimate a new generator EDMD model based on these simulations, this time using Random Fourier Features as observables⁴⁴. Figure 3, shows the eigenvalues of the generator for these cases compared to the learned generator built upon the original dataset. The result shows that learning a state-dependent diffusion is necessary to recover the original system’s leading eigenvalues. To show the scalability of the method, we repeat the analysis on a real system in the following section.

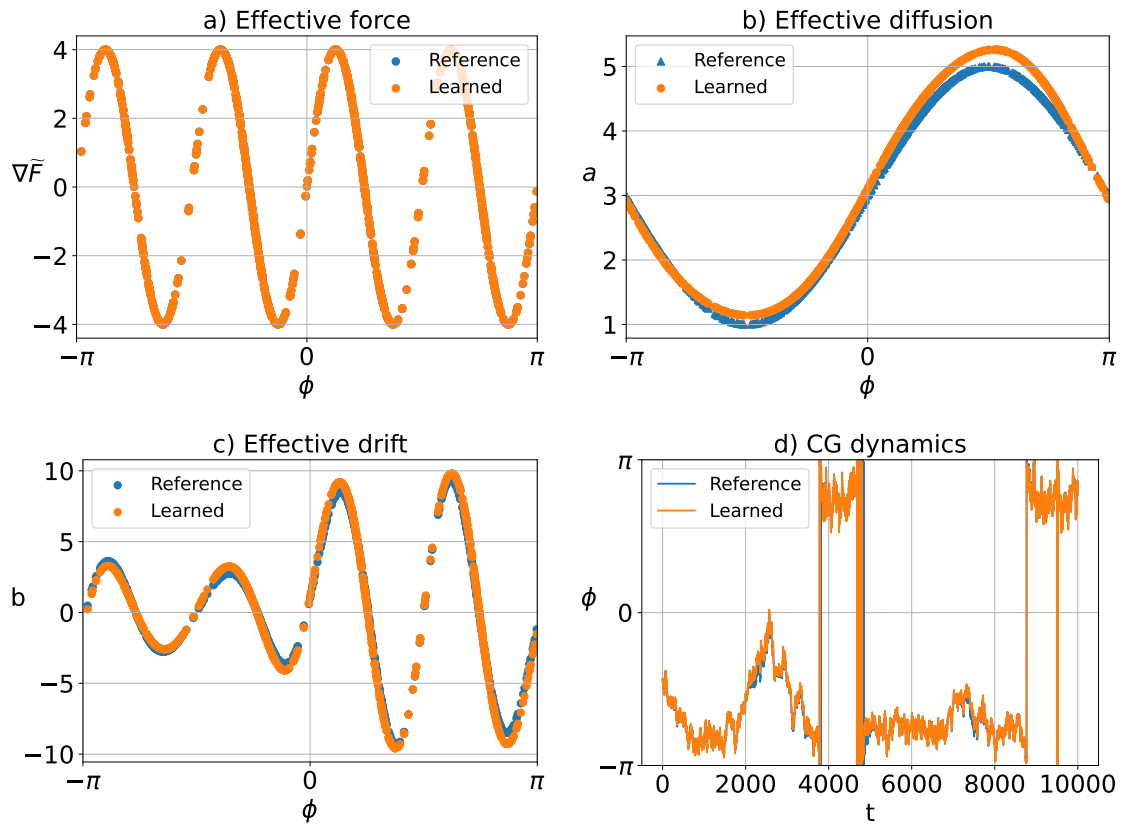


Figure 2: Application of Algorithm 1 to identify angular dynamics for the Lemon-slice system. Effective force in (a), effective diffusion in (b), effective drift in (c), and integration of an example trajectory, using both the reference and learned SDE in (d).

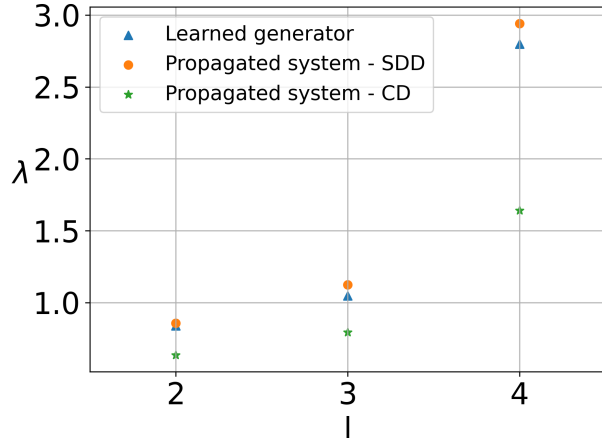


Figure 3: Dominant eigenvalues of the generator, using models built on simulation data of the learned coarse-grained dynamics with state-dependent diffusion (SDD, orange) and with constant diffusion (CD, green). As a comparison, we show the eigenvalues of the reference generator $\hat{\mathbf{L}}_r$ using the original dataset (blue triangles). Note that the first eigenvalue is omitted as it is zero.

4.2 Alanine dipeptide

4.2.1 System introduction

Alanine dipeptide is a model system widely used in method development for simulation studies of macro-molecules. Figure 4 shows the graphical representation of Alanine dipeptide. It is well known that the dynamical behavior of the molecule can be expressed in terms of the backbone dihedral angles ϕ and ψ . We generated a 500 ns simulation of the system in explicit water, including forces in the output files. The details of the simulation settings are summarized in Table 2 in appendix. From the full atomic forces, the local mean force is computed using Equation (36). In addition, we compute the local diffusion as

$$a_{\text{loc}}^{\xi}(x) = \nabla_x \xi(x) \frac{2}{\beta \gamma} M^{-1} \nabla_x \xi^{\top}(x) \quad (47)$$

where M is the diagonal mass matrix of all atoms, β is the inverse temperature, γ is the friction, and $\nabla_x \xi(x)$ is the Jacobian of dihedral angles. This way of computing the local diffusion corresponds to a reversible overdamped Langevin process in full position space,

meaning that the resulting CG model is an approximation to that same overdamped process. Fitting an overdamped model is simpler than modeling the full non-reversible underdamped Langevin process if a non-linear CG map is used. In addition, the underdamped process is expected to be close to an overdamped model in position space after a re-scaling of time. However, this also means that the eigenvalues and timescales of the overdamped model are expected to differ from the ones obtained by directly approximating the underdamped Langevin model, while the meta stable states will remain the same.

The free energy landscape of the system with respect to these two angles is shown in Figure 4.

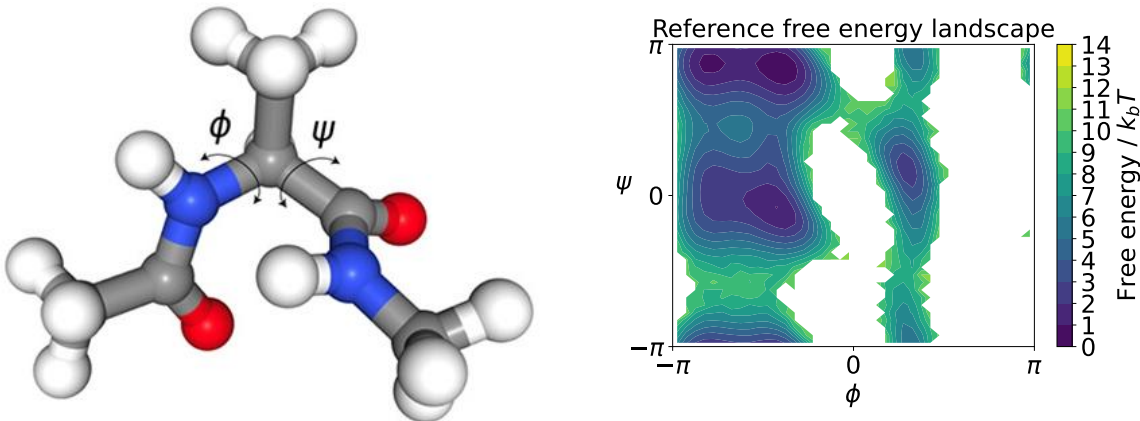


Figure 4: Graphical representation of the alanine dipeptide molecule on the left, and the reference free energy profile in two-dimensional dihedral angle space on the right.

The free energy landscape shows four minima, two on the left side, and two in the central part. We apply the kgEDMD algorithm to find the meta stable sets, and then use Algorithm 1 to learn the effective force and a state-dependent effective diffusion field in the dihedral angle space. Because of the periodicity of the CG coordinates, ϕ and ψ , we adopt the periodic Gaussian kernel. Similar to the previous example, we tune the bandwidth in the kernel function using the VAMP-score.

4.2.2 Meta stability analysis

Figure 5 a shows the leading eigenvalues of the generator obtained from the kgEDMD model. The figure indicates the four dominant eigenvalues which are corresponding to the four

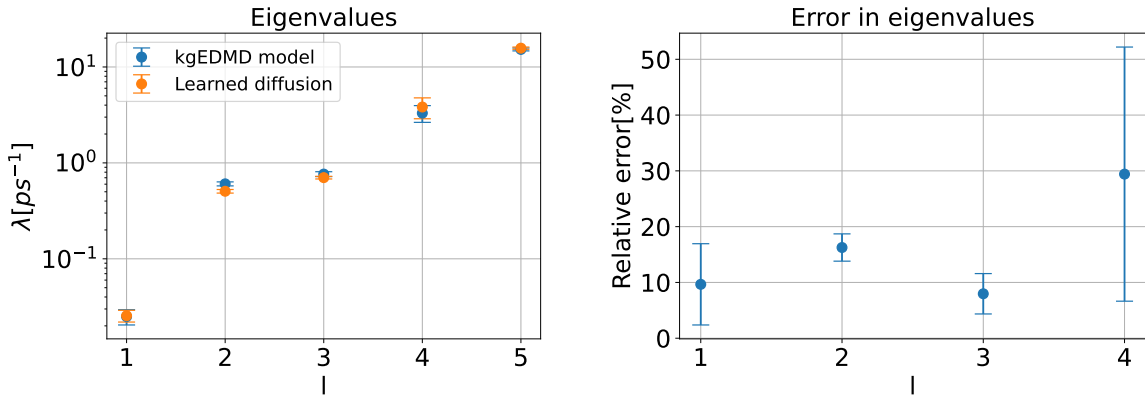


Figure 5: Approximation of generator for alanine dipeptide. The dominant eigenvalues of the reference generator $\hat{\mathbf{L}}_r$ and the learned generator $\hat{\mathbf{L}}_\alpha^\xi$ built upon the learned effective diffusion on the left, and the relative error of these eigenvalues compared to the reference is shown on the right.

minima in the free energy landscape followed by a gap. In addition, we also show the eigenvalues of the generator \mathbf{L}_α^ξ corresponding to the optimal effective diffusion, which agree well with the reference. Errorbars in the figures are generated by analyzing 5 independent subsampled sets of the original data set, each one comprising 2000 samples.

4.2.3 Identification of CG dynamics

For this 2-dimensional CG dynamics, we can express the diffusion field in a 2×2 full matrix. Here we assume though, that the learned diffusion is a diagonal matrix. Figure 6 shows the first and second diagonal terms of the learned diffusion field.

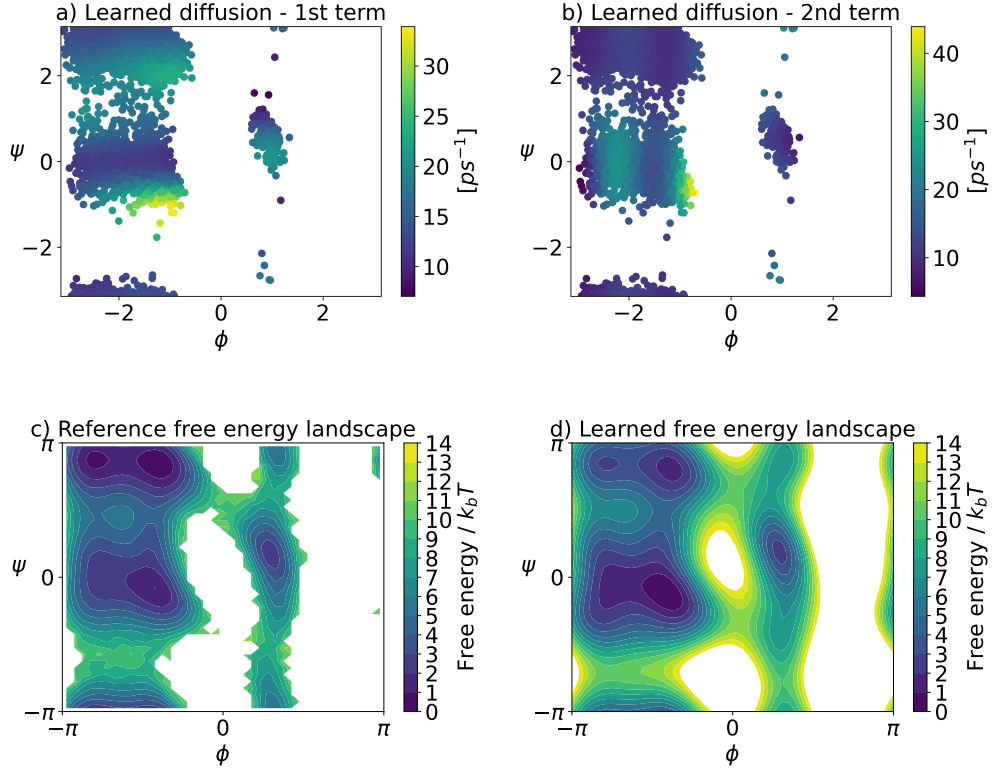


Figure 6: The first (a) and second (b) diagonal terms of the learned diffusion covariance matrix a , the reference free energy surface (c) and the free energy surface learned via kernel-based force matching (d).

For the diffusion learning process, we incorporate 2000 samples of the available dataset. The next step is to apply force matching algorithm to obtain the effective force. The reference and learned effective free energy surface are depicted in Figures 6c and 6d, respectively. It is noticeable that the learned free energy surface correctly captures all energetic minima, and approximates the energy barriers properly. We also note that $m = 50,000$ samples were required to obtain the results in Figure 6 d with kernel-based force matching.

From the effective force and diffusion, one can compute the effective drift from which the SDE governing the dynamics in the CG space can be formed. We integrate the learned SDE for a short span of time (6 ns). Figure 7 a shows the estimated free energy surface obtained from a histogram of the propagated dataset. The learned SDE reproduces the free energy

surface up to slightly higher inaccuracies sampling the upper right minimum. The four meta stable states are also correctly reproduced by a PCCA analysis of the propagated coarse grained SDE, as shown in Figure 7 b.

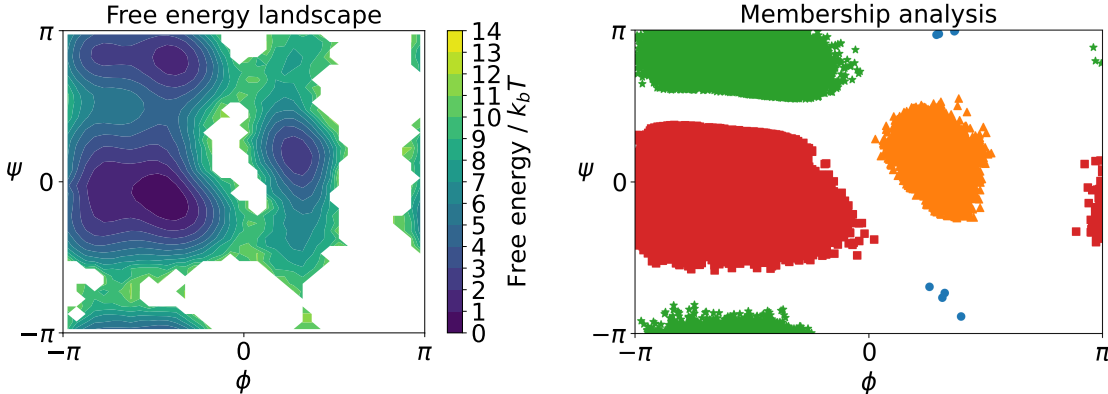


Figure 7: Propagation of the coarse grained SDE built upon learned effective force and diffusion for 6 ns. Potential energy on the left, and membership analysis on a sub-sample of propagated dynamics on the right.

In addition, we also generate a trajectory of the coarse grained SDE, but with the diffusion set to a constant. We choose the value of constant diffusion according to the average of the learned diffusion on the original dataset, resulting in $a \approx 3.8 \text{ ps}^{-1}$. For both data sets, we estimate a generator EDMD model, and show the resulting eigenvalues in Figure 8, compared to the ones corresponding to the learned generator built upon the original dataset. The result shows that the proposed coarse grained SDE with state dependent potential and diffusion (green square) successfully reproduces kinetic properties of the full-space system projected onto the CG coordinates. Moreover, one can notice that both the variable and constant diffusion fields lead to almost the same timescales. We also observe that the simulation time of 6 ns is not long enough to observe sufficient transitions into the upper right minimum, leading to inaccurate results for the fourth eigenvalue when estimated from the simulation data. This is once again due to the inaccurate estimate for the energy barrier surrounding the upper right minimum.

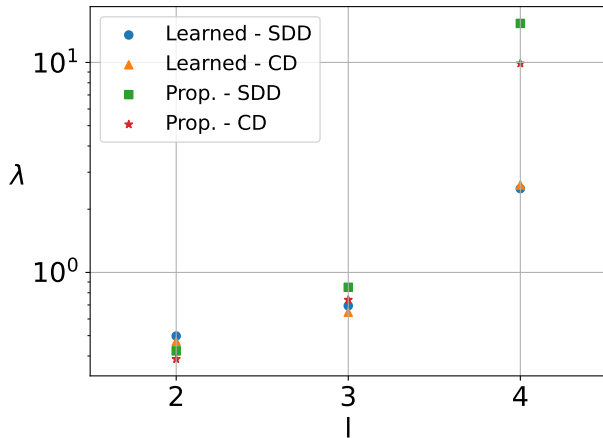


Figure 8: Dominant eigenvalues of the generator, using models built on simulation data of the learned coarse-grained dynamics with state-dependent diffusion (Prop.-SDD, green) and with constant diffusion (Prop.-CD, red). As a comparison, we show the eigenvalues of the optimal learned generator matrix $\hat{\mathbf{L}}_{\alpha}^{\xi}$, assuming either state-dependent diffusion (blue dots) or constant diffusion (orange triangles). Note that the first eigenvalue is omitted as it is zero.

5 Discussion

We presented the use of kernel-based approximation to the Koopman generator – kgEDMD – to determine meta stable sets and to learn the parameters of CG models for stochastic systems. For reversible systems, we presented a single learning pipeline to identify both the potential energy and the diffusion governing the effective SDE in CG space. By means of two examples, a two-dimensional model potential and the alanine dipeptide, we showed that the learned effective dynamics is able to reproduce both thermodynamic and kinetic quantities of the full dynamics with high accuracy.

In the molecular example, we found that the CG dynamics based on the fully state-dependent diffusion performed comparably to a constant-diffusion model using the average value of the learned diffusion. It should be noted, however, that determining this average value requires to learn the optimal state-dependent model in the first place. However, these observations can serve as a basis for a bottom-up construction of the effective diffusion, starting from a simple constant model, and increasing the complexity incrementally. Additional future

research topics include improvements to the efficiency of the method, using, for example, sparse approximations using random Fourier features⁴⁵. Moreover, one can also try to simultaneously optimize the CG mapping ξ along with the parameters of the CG model, for instance by balancing the VAMP score versus the complexity of the CG model.

Data Availability Statement

Codes and data to reproduce the results and figures shown in this manuscript are available from the following public repository: [10.5281/zenodo.13808938](https://zenodo.org/record/13808938).

6 Appendix

6.1 Notation

The most important notation used in the manuscript is summarized in Table 1.

Table 1: Overview of notation

X_t	stochastic process
k, Φ	kernel and associated feature map
\mathbb{H}	reproducing kernel Hilbert space
\mathcal{K}^τ	Koopman operator with lag time τ
\mathcal{L}	generator of the Koopman operator
\mathbf{h}	reduced basis set from whitening transformation
$\hat{\mathbf{L}}, \hat{\mathbf{L}}_r$	generator matrix and reduced generator matrix
σ_α^ξ	effective diffusion parameterized by α
$\hat{\mathbf{L}}_\alpha^\xi$	effective generator matrix for diffusion with parameters α
F, F^ξ	potential and effective potential
$f_{\text{lmf}}^\xi, a_{\text{loc}}^\xi$	local mean force and local diffusion
$\nabla_1 f$	gradient of f with respect to the first argument
$\nabla_2 f$	gradient of f with respect to the second argument
$A \cdot_{ a,b} B$	contraction of arguments a -th of A and b -th of B

6.2 VAMP-score

We tune hyper-parameters of the proposed method based on *VAMP variational principle* proposed in,²⁷ stating that for reversible systems, the k dominant eigenvalues of the Koopman generator can be obtained by a minimization problem

$$\sum_{i=1}^k \lambda_i = \min_{\phi_0, \dots, \phi_k} \sum_{i=1}^k \langle \phi_i, \mathcal{L}\phi_i \rangle_{\mu} \quad (48)$$

where the ϕ_i are orthogonal functions. We use this variational principle to optimize the kernel bandwidth in the context of our proposed method. To do this robustly and avoid overfitting, we make use of standard cross validation scheme by introducing 40% of dataset as test set. Figure 9 shows the result for the lemon slice example, using Gaussian and periodic Gaussian kernels.

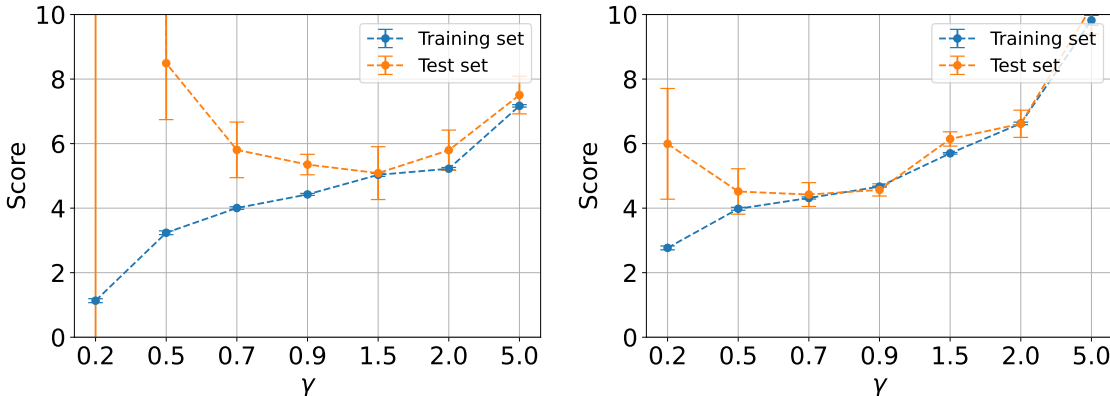


Figure 9: VAMP-score analysis for the Lemon slice example using periodic Gaussian kernel on the left and Gaussian kernel on the right

We applied the same procedure for optimizing the bandwidth for the example of alanine dipeptide. The only difference is that due to the relative complexity of this example compared to the Lemon slice, and requiring to incorporate more data for the optimization, we use random Fourier features (RFF) to reduce the size of basis functions, leading to a low-rank approximation of the generator. Figure 10 shows the result for optimization of the

bandwidth.

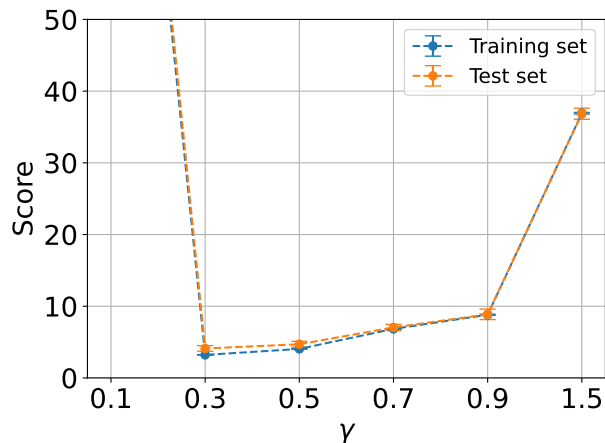


Figure 10: VAMP-score analysis for alanine dipeptide.

,

6.3 Simulation Settings for Alanine Dipeptide

For the example of alanine dipeptide, we used the Gromacs⁴⁶ simulation software to produce a 500 ns simulation. The details of the input setting we used for running the simulation is summarized in Table 2.

Table 2: Experiment setup

Force Field	AMBER99SB-ILDN
Temperature	300 K
Time constant ($1/\gamma$)	0.2 ps
Integrator	Langevin dynamics
Time step	2 fs
Simulation time	500 ns
Export data frequency	100 fs

References

- (1) Frenkel, D.; Smit, B. *Understanding molecular simulation: from algorithms to applications*, 3rd ed.; Elsevier, 2023.
- (2) Onuchic, J. N.; Luthey-Schulten, Z.; Wolynes, P. G. Theory of protein folding: the energy landscape perspective. *Annual review of physical chemistry* **1997**, *48*, 545–600.
- (3) Karplus, M.; Petsko, G. A. Molecular dynamics simulations in biology. *Nature* **1990**, *347*, 631–639.
- (4) Sidky, H.; Chen, W.; Ferguson, A. L. Machine learning for collective variable discovery and enhanced sampling in biomolecular simulation. *Molecular Physics* **2020**, *118*.
- (5) Das, P.; Moll, M.; Stamati, H.; Kaviraki, L. E.; Clementi, C. Low-dimensional, free-energy landscapes of protein-folding reactions by nonlinear dimensionality reduction. *Proceedings of the National Academy of Sciences* **2006**, *103*, 9885–9890.
- (6) Clementi, C. Coarse-grained models of protein folding: toy models or predictive tools? *Current opinion in structural biology* **2008**, *18*, 10–15.
- (7) Rohrdanz, M. A.; Zheng, W.; Clementi, C. Discovering Mountain Passes via Torchlight: Methods for the Definition of Reaction Coordinates and Pathways in Complex Macromolecular Reactions. *Annual Review of Physical Chemistry* **2013**, *64*, 295–316.
- (8) Wang, J.; Ferguson, A. Nonlinear machine learning in simulations of soft and biological materials. *Molecular Simulation* **2018**, *44*, 1090–1107.
- (9) John, S.; Csányi, G. Many-body coarse-grained interactions using Gaussian approximation potentials. *The Journal of Physical Chemistry B* **2017**, *121*, 10934–10949.
- (10) Zhang, L.; Han, J.; Wang, H.; Car, R., et al. DeePCG: Constructing coarse-grained models via deep neural networks. *The Journal of chemical physics* **2018**, *149*.

- (11) Wang, J.; Olsson, S.; Wehmeyer, C.; Pérez, A.; Charron, N. E.; de Fabritiis, G.; Noé, F.; Clementi, C. Machine Learning of Coarse-Grained Molecular Dynamics Force Fields. *ACS Central Science* **2019**, *5*, 755–767.
- (12) Legoll, F.; Lelièvre, T. Effective dynamics using conditional expectations. *Nonlinearity* **2010**, *23*, 2131–2163.
- (13) Zhang, W.; Hartmann, C.; Schütte, C. Effective dynamics along given reaction coordinates, and reaction rate theory. *Faraday discussions* **2016**, *195*, 365–394.
- (14) Schneider, E.; Dai, L.; Topper, R. Q.; Drechsel-Grau, C.; Tuckerman, M. E. Stochastic neural network approach for learning high-dimensional free energy surfaces. *Physical review letters* **2017**, *119*, 150601.
- (15) Noid, W. G.; Chu, J.-W.; Ayton, G. S.; Krishna, V.; Izvekov, S.; Voth, G. A.; Das, A.; Andersen, H. C. The multiscale coarse-graining method. I. A rigorous bridge between atomistic and coarse-grained models. *The Journal of Chemical Physics* **2008**, *128*, 244114.
- (16) Davtyan, A.; Voth, G. A.; Andersen, H. C. Dynamic force matching: Construction of dynamic coarse-grained models with realistic short time dynamics and accurate long time dynamics. *The Journal of Chemical Physics* **2016**, *145*.
- (17) Bereau, T.; Rudzinski, J. F. Accurate Structure-Based Coarse Graining Leads to Consistent Barrier-Crossing Dynamics. *Phys. Rev. Lett.* **2018**, *121*, 256002.
- (18) Davies, E. B. Metastable States of Symmetric Markov Semigroups II. *Journal of the London Mathematical Society* **1982**, *s2-26*, 541–556.
- (19) Dellnitz, M.; Junge, O. On the approximation of complicated dynamical behavior. *SIAM J. Numer. Anal.* **1999**, *36*, 491–515.

- (20) Schütte, C.; Fischer, A.; Huisinga, W.; Deuffhard, P. A direct approach to conformational dynamics based on hybrid Monte Carlo. *J. Comput. Phys.* **1999**, *151*, 146–168.
- (21) Klus, S.; Nüske, F.; Koltai, P.; Wu, H.; Kevrekidis, I.; Schütte, C.; Noé, F. Data-Driven Model Reduction and Transfer Operator Approximation. *Journal of Nonlinear Science* **2018**, *28*, 985–1010.
- (22) Prinz, J.-H.; Wu, H.; Sarich, M.; Keller, B.; Senne, M.; Held, M.; Chodera, J. D.; Schütte, C.; Noé, F. Markov models of molecular kinetics: Generation and validation. *The Journal of Chemical Physics* **2011**, *134*, 174105.
- (23) Sarich, M.; Noé, F.; Schütte, C. On the approximation quality of Markov state models. *Multiscale Model. Simul.* **2010**, *8*, 1154–1177.
- (24) Bowman, G. R., Pande, V. S., Noé, F., Eds. *An Introduction to Markov State Models and Their Application to Long Timescale Molecular Simulation*; Springer Netherlands, 2014; Vol. 797.
- (25) Noé, F.; Nüske, F. A variational approach to modeling slow processes in stochastic dynamical systems. *Multiscale Modeling and Simulation* **2013**, *11*, 635–655.
- (26) Mardt, A.; Pasquali, L.; Wu, H.; Noé, F. VAMPnets for deep learning of molecular kinetics. *Nature Communications* **2018**, *9*.
- (27) Wu, H.; Noé, F. Variational approach for learning Markov processes from time series data. *Journal of Nonlinear Science* **2020**, *30*, 23–66.
- (28) Nüske, F.; Boninsegna, L.; Clementi, C. Coarse-graining molecular systems by spectral matching. *Journal of Chemical Physics* **2019**, *151*.
- (29) Klus, S.; Nüske, F.; Peitz, S.; Niemann, J.-H.; Clementi, C.; Schütte, C. Data-driven approximation of the Koopman generator: Model reduction, system identification, and control. *Physica D: Nonlinear Phenomena* **2020**, *406*, 132416.

- (30) Wendland, H. *Scattered Data Approximation*; Cambridge University Press, 2004.
- (31) Christmann, A.; Steinwart, I. *Support Vector Machines*; Springer New York, 2008.
- (32) Klus, S.; Nüske, F.; Hamzi, B. Kernel-based approximation of the Koopman generator and Schrödinger operator. *Entropy* **2020**, *22*, 722.
- (33) Pavliotis, G. A. Stochastic processes and applications. *Texts in Applied Mathematics* **2014**, *60*.
- (34) Koopman, B. O. Hamiltonian systems and transformation in Hilbert space. *Proc. Natl. Acad. Sci. U S A* **1931**, *17*, 315.
- (35) Mezić, I. Spectral Properties of Dynamical Systems, Model Reduction and Decompositions. *Nonlinear Dynamics* **2005**, *41*, 309–325.
- (36) Lelièvre, T.; Stoltz, G. Partial differential equations and stochastic methods in molecular dynamics. *Acta Numerica* **2016**, *25*, 681–880.
- (37) Schmid, P. J. Dynamic mode decomposition of numerical and experimental data. *Journal of Fluid Mechanics* **2010**, *656*, 5–28.
- (38) Budišić, M.; Mohr, R.; Mezić, I. Applied Koopmanism. *Chaos: An Interdisciplinary Journal of Nonlinear Science* **2012**, *22*.
- (39) Mauroy, A., Mezić, I., Susuki, Y., Eds. *The Koopman Operator in Systems and Control*; Springer International Publishing, 2020; Vol. 484.
- (40) Williams, M. O.; Kevrekidis, I. G.; Rowley, C. W. A Data-Driven Approximation of the Koopman Operator: Extending Dynamic Mode Decomposition. *Journal of Nonlinear Science* **2015**, *25*, 1307–1346.
- (41) Duvenaud, D. Automatic model construction with Gaussian processes. Ph.D. thesis, 2014.

- (42) Nüske, F.; Koltai, P.; Boninsegna, L.; Clementi, C. Spectral properties of effective dynamics from conditional expectations. *Entropy* **2021**, *23*, 134.
- (43) Deuffhard, P.; Weber, M. Robust Perron cluster analysis in conformation dynamics. *Linear Algebra Appl* **2005**, *398*, 161–184.
- (44) Nüske, F.; Klus, S. Efficient approximation of molecular kinetics using random Fourier features. *The Journal of Chemical Physics* **2023**, *159*, 074105.
- (45) Nüske, F.; Klus, S. Efficient approximation of molecular kinetics using random Fourier features. *The Journal of Chemical Physics* **2023**, *159*.
- (46) Bekker, H.; Berendsen, H.; Dijkstra, E.; Achterop, S.; Vondrumen, R. v.; Vander-spoel, D.; Sijbers, A.; Keegstra, H.; Renardus, M. Gromacs-a parallel computer for molecular-dynamics simulations. 4th international conference on computational physics (PC 92). 1993; pp 252–256.